Observations of Intermittent Chaos in Plasmas

P. Y. Cheung, S. Donovan, and A. Y. Wong
Department of Physics, University of California, Los Angeles, California 90024-1547
(Received 13 June 1988)

The transition to chaos through intermittency has been observed in a steady-state plasma system. Results from real-time signals, spectral analysis, and constructed Poincaré sections are used to confirm the existence of intermittency. Low-frequency $1/f$-type noise is also observed during the onset of chaos.

PACS numbers: 52.25.Gj, 05.40.+j, 05.45.+b, 52.35.Ra

The subject of order and chaos in dissipative systems has been of intense interest in recent years.[1-3] The onset of chaos has been observed in various physical systems and several routes to chaos have been identified.[4] Recently, period doubling and chaotic behavior have been observed in a pulsed plasma system.[5] In this Letter, we would like to report experimental results of the onset of chaos in a steady-state plasma system through intermittency. This is characterized by a time signal with long periods of regular or laminar oscillations interrupted by relatively short random bursts.[6] The observed intermittency displays certain features of "type-1" intermittency first introduced by Pomeau and Manneville.[7] In particular, both the temporal evolution of the oscillations and the occurrence of $1/f$-type noise[8,9] indicate that the observed intermittency is that of type 1. Although intermittent chaos has been observed in other physical systems,[10] we believe this is the first time that such phenomena have been observed in plasmas.

The mechanism for type-1 intermittency is believed to arise from a tangent bifurcation that involves the loss of stability of a periodic attractor (stable fixed point).[7,11] After bifurcation, a "ghost" of the previously stable attractor remains. This destabilized attractor attracts phase trajectories in one direction while repelling them in the other. As a result, trajectories remain near the unstable fixed point until they escape and wander in phase space. If represented on a one-dimensional return map (i.e., a map of x_n vs x_{n+1}, where x_n is a dynamic variable), successive iterations of phase trajectories form a narrow constriction of "channel" on the map.[11] In real-time signals, this constitutes periods of laminar oscillations interrupted by the intermittent occurrence of chaotic bursts.

The experiments are performed in an unmagnetized plasma device consisting of an electron-emitting cathode (a ring-shaped array of tungsten filaments) at one end and a current-collecting anode (tantalum disk, 6 cm diameter) at the other end [Fig. 1(a)]. The anode disk is mounted on a probe shaft so that the separation between the anode and cathode, d, can be varied. The cathode is connected to the chamber wall and is electrically grounded. When the anode is biased positively with respect to the cathode, energetic electrons are extracted from the cathode. The electrons partially ionize the background neutral gas and create a plasma between the cathode and the anode. As a result of the relationship between the emission of primary electrons by the cathode and the production of plasma, the two processes are coupled. The primary electrons ionize the gas and substain the plasma while the plasma reduces negative space charge and facilitates cathode emission. By varying plasma discharge parameters, one can control this coupling or feedback process and the resulting plasma can be unstable. This regime occurs when the plasma potential is negative with respect to the anode.[5] For d less than some critical value d_c, the potential profile is unstable and current oscillations occur.[12,13] In this case, the plas-

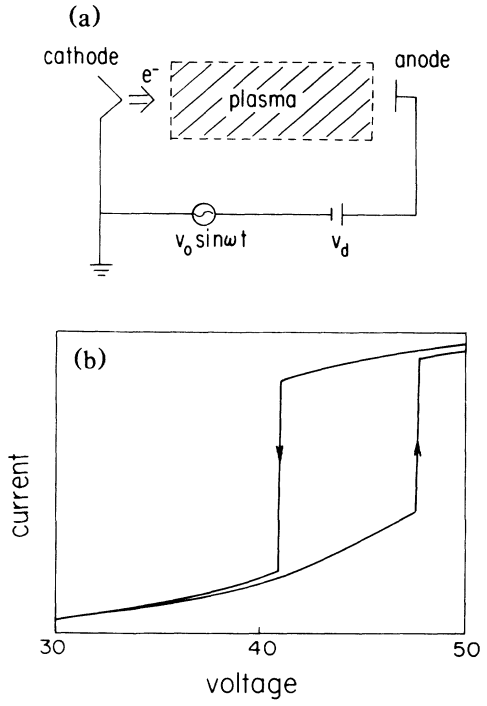

FIG. 1. (a) Schematic of experimental setup. (b) I-V characteristic of anode current, I_a, vs dc anode voltage bias, V_d. The upwards pointing arrow indicates the rapid increase in I_a as V_d is increased and the downwards pointing arrow indicates the rapid decrease in I_a as V_d is decreased.

ma can exhibit another route to chaos involving quasiperiodicity and frequency locking.[14] These results will be published elsewhere. In this Letter, we shall focus on the results where the potential does not oscillate. Typical plasma parameters are $n_0 = 10^8$–10^9 cm^{-3} and $T_e = 1$–3 eV where n_0 and T_e are the plasma density and electron temperature, respectively.

A good indication that the system may become chaotic is the occurrence of hysteresis and negative differential resistance in the current-voltage (I-V) characteristic.[15,16] This is shown in Fig. 1(b) as the anode current, I_a, plotted against the dc anode voltage bias, V_d, for a given d with no sinusoidal drive. Between $V_d = 40.8$ and 47.5 V, the I-V curve displays two sharp discontinuities and does not retrace itself. As V_d is increased from zero, the current increases smoothly and follows the lower branch of the I-V curve. At $V_d = 47.5$ V, the current makes an abrupt jump to the upper branch of the curve. If V_d is now decreased, the current decreases monotonically, following the upper branch of the curve until $V_d = 40.8$ V, where it abruptly falls to the lower branch. Within this voltage range, the system is nonlinear with

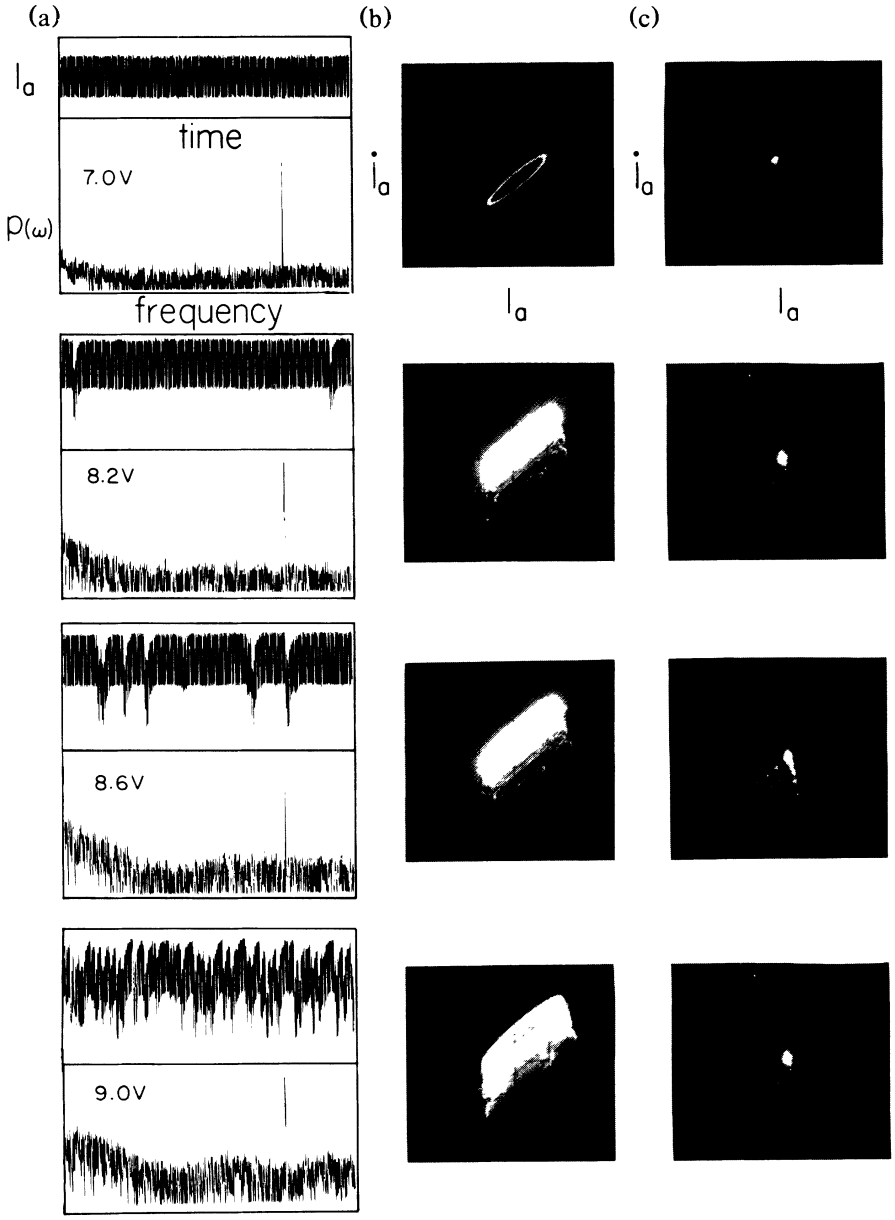

FIG. 2. (a) Real-time signals of I_a oscillations and the corresponding FFT spectra for $V_0 = 7$, 8.2, 8.6, and 9 V, respectively. The external drive frequency is at $f_o = 14.4$ kHz. The vertical scale on each FFT spectrum is logarithmic. (b) Corresponding phase-space plots of I_a vs $\dot{I}_a$ as V_0 is increased. (c) Corresponding Poincaré sections of I_a vs $\dot{I}_a$ as V_0 is increased.

multiple steady states and the I-V curve displays negative differential resistance. When the current is on the lower branch of the I-V curve, the plasma potential is negative with respect to the anode. This is the regime where the plasma can be driven to chaos. When $V_d \geq 47.5$ V, the plasma potential is positive with respect to the anode and no chaotic behavior has been observed.

To initiate intermittency, a sinusoidal signal, $V_0 \sin(2\pi f_o t)$, is applied to the anode (through a 3:1 transformer) in addition to V_d. The total anode bias, V_a, has both dc and ac components with $V_a = V_d + 3V_0 \sin(2\pi f_o t)$. The total anode current also consists of both dc and ac components. The optimum frequency f_o is approximately the inverse of ion transit time across d. The temporal evolution of I_a is monitored as V_0 is varied (maintaining all other system parameters constant). A typical sequence to chaos is demonstrated in Fig. 2(a) with $f_o = 14.4$ kHz and $V_0 = 7$, 8.2, 8.6, and 9 V, respectively. The corresponding fast Fourier transform (FFT) spectra are also displayed. Each time record displays about 400 cycles of I_a and is only a portion of the entire time record (2000 cycles) over which the FFT is performed. At $V_0 = 7$ V, only laminar current oscillations are observed and the power spectrum shows a sharp peak at f_o. As V_0 increases to 8.2 V, long periods of laminar current oscillations are interrupted by irregular jumps in I_a. The spectrum now shows a strong enhancement of low-frequency noise (to be discussed in detail later). When $V_0 = 8.6$ V, the laminar periods become shorter as intermittent jumps in I_a occur more often. Finally, at $V_0 = 9$ V, the system is chaotic. The temporal evolution of I_a from laminar oscillations to chaos is similar to the type-1 intermittency observed in other physical systems.[10]

The above transition to chaos can also be represented as a sequence of phase-space plots. This is done by displaying both I_a and their differentiated values, $\dot{I}_a$, on an oscilloscope in the x-y mode. The results are shown in Fig. 2(b). Phase-space trajectories are observed to deform from nice limit cycles (at small V_0) to complex, nested patterns (at large V_0) when the system is chaotic.

The complicated phase-space plots can be simplified through the construction of Poincaré sections[11] that retain the same topological characteristics as the original plots. Mathematically, the Poincaré sections are formed through the intersections of phase-space trajectories with an arbitrary plane S. The resultant sections reduce the number of coordinates by one, simplifying the original continuous trajectories to discrete mappings. Physically, this is done by strobing the oscilloscope at f_o and at a fixed relative phase ϕ_0. The results are shown in Fig. 2(c). At $V_0 = 7$ V, the resultant Poincaré map contains only a single point since the current oscillations are laminar. As V_0 increases to 8.2 V, the single point begins to elongate into a continuous line segment with a few scattered points now appearing on the map. The elongated line segment represents the continuous phase slippage between successive laminar periods as trajectories pass through the narrow channel formed near the unstable fixed point. The scattered points on the Poincaré map are due to trajectories that have escaped briefly from the channel and wandered chaotically through phase space. At $V_0 = 8.6$ V, the narrow channel has now been widened and phase trajectories quickly pass the unstable fixed point, spending as much time outside the channel as inside. At $V_0 = 9$ V, the resultant Poincaré map consists of randomly scattered points.

As discussed earlier, the power spectra shows strong enhancement of $1/f$-type low-frequency noise[8] as intermittency occurs. For example, broadband spectral power enhancement of 20 dB or more at $f \sim 1$ kHz is typically observed with $f_o = 14.4$ kHz. To measure the spectral power scaling with frequency accurately, noise spectra data are first corrected to compensate for inherent low-frequency system-noise pickup (e.g., 60 Hz noise from power supplies). The resultant dependence of low-frequency noise enhancement on frequency is displayed on a log-log plot shown in Fig. 3 for $V_0 = 8.6$ V. At the onset of chaos, a power-law spectrum is observed with a scaling relationship of $f^{-2.1 \pm 0.2}$ for $f \geq 1$ kHz. This scaling agrees with results from numerical simulations of type-1 intermittency where Lorentzian spectra with f^{-2} scaling were observed.[9,17] Such spectra are also common in systems displaying random processes with long relaxation times. As a result, the occurrence of intermittency with a Lorentzian spectrum in the present system can be explained in terms of induced hopping between two plasma states by the external drive.

Below $f \sim 1$ kHz, the above scaling no longer holds. The noise power is observed to be almost constant with frequency. This is due to perturbations by inherent thermal (white) plasma noise that causes arbitrarily long laminar periods to become finite and intermittent bursts to occur more often.[9]

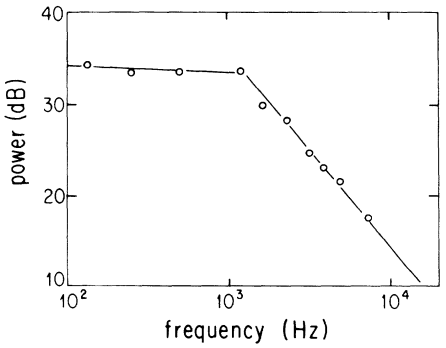

FIG. 3. Low-frequency spectral noise power dependence on frequency. The data are the same as the low-frequency portion of the FFT spectrum presented in Fig. 2 for $V_0 = 8.6$ V but are replotted on a log-log plot.

Similar behavior has been observed in numerical simulations of nonlinear differential equations. In particular, intermittency, $1/f$-type noise, and chaos have been observed in simulations with the forced-Duffing equation.[18]

In summary, the intermittent route to chaos has been identified in a plasma system. Results from real-time signals, spectral analysis, and constructed Poincaré sections of anode current oscillations are used to confirm the existence of intermittency. Low-frequency noise that scales $\sim f^{-2}$ has been observed at the onset of chaos and the particular intermittent route observed displays certain characteristics that are similar to that of type-1 intermittency.

The authors would like to acknowledge technical assistance by Onnik Soghomonian. This research was supported by the National Science Foundation under Grant No. PHY87-19129 and one of the authors (S.D.) was supported partially by the National Science Foundation-REU program.

[1]Edward Ott, Rev. Mod. Phys. **53**, 643 (1981).

[2]J. P. Eckmann, Rev. Mod. Phys. **53**, 655 (1981).

[3]M. J. Feigenbaum, J. Stat. Phys. **19**, 25 (1978).

[4]Harry L. Swinney, Physica (Amsterdam) **7D**, 3 (1983).

[5]P. Y. Cheung and A. Y. Wong, Phys. Rev. Lett. **59**, 551 (1987).

[6]Paul Manneville and Yves Pomeau, Physica (Amsterdam) **1D**, 219 (1980).

[7]Yves Pomeau and Paul Manneville, Commun. Math. Phys. **74**, 189 (1980).

[8]P. Dutta and P. M. Horn, Rev. Mod. Phys. **53**, 497 (1981).

[9]A. Ben-Mizarchi, I. Procaccia, N. Rosenberg, and A. Schmidt, Phys. Rev. A **31** 1830 (1985).

[10]P. Bergé, M. DuBois, P. Manneville, and Y. Pomeau, J. Phys. (Paris), Lett. **41**, 341 (1980); Y. Pomeau, J. C. Roux, A. Rossi, S. Bachelart, and C. Vidal, J. Phys. (Paris), Lett. **42**, 271 (1981).

[11]Pierre Bergé, Yves Pomeau, and Christian Vidal, *Order within Chaos* (Wiley, New York, 1986).

[12]P. Leung, A. Y. Wong, and B. Quon, Phys. Fluids **23**, 992 (1980); P. L. Gray, S. Kuhn, T. L. Crystal, and C. K. Birdsall, in *Proceedings of Second Symposium on Plasma Double Layers and Related Topics,* edited by R. Schrittwieser and G. Eder (Institute of Theoretical Physics, Innsbruck, Austria, 1984).

[13]Peter Burger, J. Appl. Phys. **36**, 1938 (1965); W. T. Norris, J. Appl. Phys. **35**, 3260 (1964).

[14]Per Bak, Tomas Bohr, and Mogens Høgh Jensen, Phys. Scr. **T9**, 50 (1985).

[15]S. W. Teitsworth and R. M. Westervelt, Physica (Amsterdam) **23D**, 181 (1986); A. B. Pippard, *The Physics of Vibrations* (Cambridge Univ. Press, New York, 1978), Vol. 1.

[16]B. K. Ridley, Proc. Phys. Soc. London **82**, 954 (1963).

[17]E. G. Gwinn and R. M. Westervelt, Phys. Rev. A **33**, 4143 (1986).

[18]Yoshisuke Ueda and Norio Akamatsu, IEEE Trans. Circuits Syst. **28**, 217 (1981).

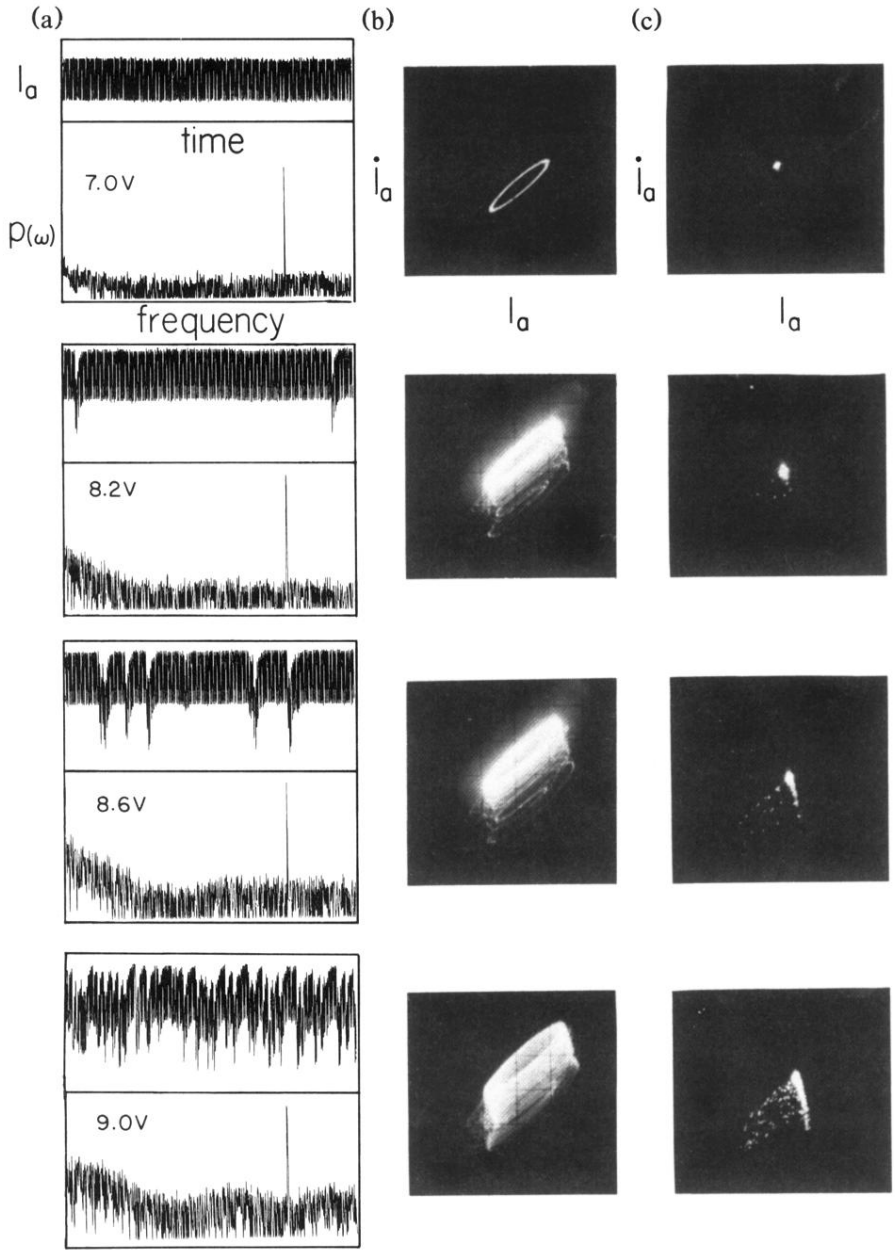

FIG. 2. (a) Real-time signals of I_a oscillations and the corresponding FFT spectra for $V_0=7$, 8.2, 8.6, and 9 V, respectively. The external drive frequency is at $f_o=14.4$ kHz. The vertical scale on each FFT spectrum is logarithmic. (b) Corresponding phase-space plots of I_a vs $\dot{I}_a$ as V_0 is increased. (c) Corresponding Poincaré sections of I_a vs $\dot{I}_a$ as V_0 is increased.